Spatial Distribution of Acoustic Emissions of Rock Salt under Different Stress Conditions

Mingming Xu[1,2], Jianfeng Liu[1,2,3], Dewen Zheng[4], Liang Chen[5], Zhide Wu[4], Lina Ran[4], Michael Zhengmeng Hou[6], Yang Gou[6], and Huining Xu[1,2]

[1] State Key Laboratory of Hydraulics and Mountain River Engineering, Sichuan University, Chengdu 610065, China
[2] State Key Laboratory of Geohazard Prevention and Geoenvironment Protection, Chengdu University of Technology, Chengdu 610059, China
[3] Key Lab. of Energy Engineering, Safety and Mechanics on Disasters (Sichuan Univ.), Ministry of Education, Chengdu, 610065, China
[4] Langfang Branch, Research Institute of Petroleum Exploration and Development, Langfang 065007, China
[5] Beijing Research Institute of Uranium Geology, Beijing 100029, China
[6] Institute of Petroleum Engineering, Clausthal University of Technology, Clausthal-Zellerfeld 38678, Germany

Abstract. In this paper, the study on the spatial distribution of acoustic emission (AE) events in rock salt under different stress conditions was reported. The study showed that under indirect tensile stress condition, the AE events were mainly induced by the stress concentration near the loading surface and by intergranular deformation before rock failure, while during failure and the post-failure process the AE events were essentially related to the damage development, especially near the tensile failure surface. Under uniaxial compressive stress condition, the closure of initial micro-cracks including those artificially produced during coring and sample preparation and intergranular deformation were the main mechanisms responsible for the occurrence of AE events at the initial_deformation stage, and then transferred to damage development until the post-failure stage was met. In triaxial compression tests, the influence of the closure of initial micro-cracks and intergranular deformation was still the main cause for AE events at the confining pressure loading stage and the initial axial loading stage. However, the influence of plastic deformation becomes more pronounced at the plastic yield stage and the post-peak stage. Intensive occurrence and accumulation of AE events before rock failure was noticed under different stress conditions. In indirect tensile tests, the recorded AE events were mainly accumulated along the failure surface. However, this reasonable phenomenon was not evident in uni- and triaxial compression tests, where the spatial distribution is generally homogeneous.

Keywords: rock salt, indirect tension, uniaxial compression, triaxial compression, AE spatial distribution.

M.Z. Hou et al. (Eds.): *Clean Energy Systems in the Subsurface*, SSGG, pp. 329–339.
DOI: 10.1007/978-3-642-37849-2_27

1 Introduction

Due to its low permeability, self-sealing capacity, and outstanding practicability of mining activities, rock salt is internationally considered as an ideal host rock for gas/oil underground storage and radioactive waste repositories. Extensive studies have been carried out on the mechanical properties of rock salt and various results were achieved [1-7].

As an important non-destructive monitoring method, the acoustic emission (AE) monitoring technique is widely used to investigate the damage evolution and rock failure process. For instance, Obert [8] and Hodgson [9] used the AE monitoring method to identify the failure position during the excavation of underground structures. Li [11] confirmed the validity of the Kaiser Effect [10] for rock. Filimonov[12-13] revealed that the acoustic emission is stronger in rock salt than in clay rock and shale, and obtained the effect of the loading rate on AE properties. Alkan[14] studied the dilation properties of rock salt under triaxial compressive conditions. Based on experimental investigation, Liu et al. [15-17] established the relationship between fractal dimensions of AE events spatial distribution and the energy release in indirect tensile and uniaxial compression tests. Based on these investigations, the relationship between the recorded AE events and the deformation as well as the failure states of rock salt have been systematically studied. However, little attention has been given to the formation mechanism of the AE distribution during the whole loading process under different stress conditions.

In this paper, through a series of experimental investigations under different stress conditions the full process of rock salt failure in direct tensile tests, uniaxial compression tests and triaxial compression tests, respectively, is analyzed by the characterization of AE distribution.

2 Test Equipments and Methods

2.1 Test Equipments and Rock Samples

The test equipment consists of a MTS815 Flex Test GT rock test system and a 3D AE monitoring system of PCI-II (Fig. 1). The maximum axial loading is 4600 kN, and the maximum confining pressure and pore pressure are both 140 MPa. The PCI-II AE system includes 8 channels for the spatial AE-detection. The central frequency of AE sensors is 300 kHz. 8 AE sensors were installed symmetrically in a radial direction along the cylinder surface and the distance from the sensor to the nearest end surface is about 10 mm for uniaxial compression tests. For indirect tensile tests, the sensors were placed on both sides of the possible tensile failure surface and the distance between the sensor and the circle edge is about 2 mm. For triaxial compression tests, the sensors were placed on the outside of the triaxial cell. There were 4 sensers for each end of the specimen surface, respectively.

The rock samples were taken at a depth of 500 m in Anning, Yunnan Province of China. Following the "Standards of the engineering rock test methods" (GB/T50266–99) [18] and "Standards of rock test for water conservancy and hydroelectric power" (SL264-2001) [19], the samples were prepared using the dry lathing method. The sample size of indirect tension and compression tests were D90×H50mm and D90×H200mm, respectively. The samples had an average salt content of up to 79%.

Fig. 1 MTS815 Flex Text GT rock mechanics test system

2.2 Test Methods

For indirect tensile tests, namely the Brazil split tests, the loading process was controlled by axial displacement (LVDT). The loading rate was 0.05 mm/min before peak stress, and then transferred to 0.1 mm/min until rock failure. For uniaxial compression tests, the axial loading rate was 30 kN/min from the start of loading until the elastic deformation finished; then, the loading was transferred to LVDT control, with a loading rate of 0.1mm/min. For triaxial compression tests, the axial loading process was also controlled by axial displacement with a loading rate of 1.0mm/min, and the loading rate for confining pressure was 3.0 MPa/min. In all of the above tests, the testing temperature was room temperature (25°C).

3 Test Results and Analysis

3.1 AE Events Properties for Indirect Tensile Tests

The recorded AE events were categorized according to axial stress increments. For instance, the inserted graph "20~40%" in Fig. 2 showed the recorded AE events and their spatial distribution of the stress increment between 20% to 40% of the peak stress. While the increment "100~60%" depicts the recorded AE events from 100% to 60% of peak stress at the post-failure stage.

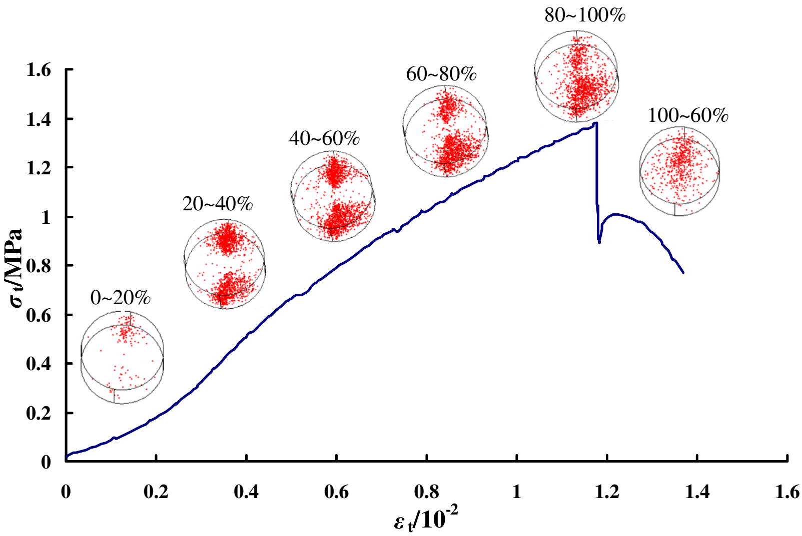

Fig. 2 Spatial distribution of AE events of rock salt for indirect tensile test

In Fig. 2, due to the stress concentration around the loading surface, it was noticed that the AE events were recorded along the lines of loading contact points of rock sample at the beginning of the loading process, and finally expanded to the central part. The number and distribution of recorded AE events were similar at the stages "20~40%", "40~60%" and "60~80%". In these phases, the occurrences of AE events were mainly induced by damage development near the loading surface and relative deformation between grains. However, with the increase of tensile stresses, the influence of stress concentration at the contact lines became less evident and the damage development became more dominant for AE events, presented at the stage "80~100%". This is concluded from the result, where the recorded AE events were mainly located near the failure surface in the central part of the rock sample. The distribution of recorded AE events and the provoking process remained dominant at the post-failure stage (100-60%) of the peak stress.

Fig. 2 also presents the overall accumulation process of AE events along the failure surface, and the evolution process of the initiation, propagation and coalescence of micro-cracks during indirect tensile tests. According to the test results of 5 specimens, the maximal and minimal tensile strength of rock salt was 1.52 MPa and 1.30 MPa, respectively. The average tensile strength was 1.38 MPa.

Fig. 3 showed the corresponding final failure pattern and AE distribution of the test presented in Fig. 2. It indicated that the failure surface expanded along the loading line (dashed line) in Fig. 3(a), and inclined slightly to the right on the other side, as presented in Fig. 3(b). As a result, the distribution of recorded AE events (Fig. 3(c), seen from the sample's back side) is not symmetric, thus many AE events appeared on the right side. The distribution state of AE events in Fig. 3(c), is in accordance with the failure state in Fig 3(b).

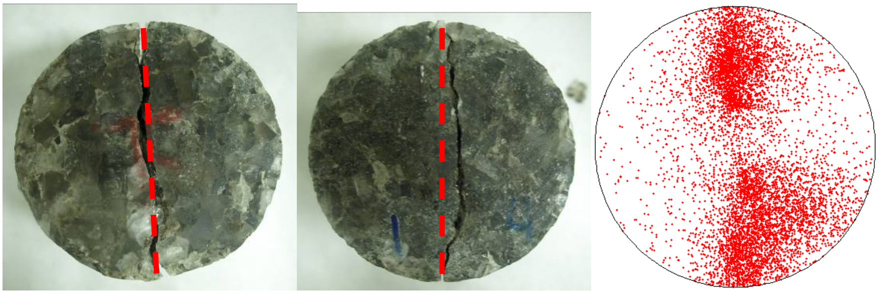

（a） sample front （b） sample rear （c） location of acoustic emissions

Fig. 3 Failure state and AE spatial distribution for indirect tensile test

3.2 AE Events Properties for Uniaxial Compression Tests

As shown in Fig. 4, during uniaxial compression tests, the recorded AE events were mainly accumulated around the loading surface at the beginning of loading process, in a cone-shape and inverted cone-shape pattern. The stress distribution in the rock sample was strongly influenced by the end restraint effect at this stage, and the AE events were essentially induced by the closure of original micro-cracks and relative deformation between grains. With the increase of axial stress, the AE events expanded to the central part, which indicated that internal damage had taken place. At the following stages, with the damage development, the accumulations of AE events were mainly located in the central and the lower part, and the influence of end restraint effect had already become quite low. At the post-failure stage ("100-80 %"), the recorded number of AE events was less than those at the peak stress stage.

Since rock salt is a typical crystallized sedimentary rock, not only the propagation and coalescence of micro-cracks, but also the friction and relative deformation between grains can generate acoustic emission. As a result, the accumulation of AE events along a certain failure surface is not as evident as observed in indirect tensile tests. Under uniaxial compressive conditions, numerous micro-cracks were generated during rock salt failure, in contrast to a single macroscopic failure surface in Brazil split tests. The average compressive strength was 25.17 MPa, which is generally approx. one order of magnitude higher than the tensile strength.

Fig. 5 shows the final failure pattern and the location of AE events after uniaxial compression. Due to the existence of argillaceous impurities in the upper part of the sample, the rock salt purity of the upper part is less than that of the lower part. As a result, in the lower part, the rock becomes more brittle and stronger than in the upper part [20], so the rock failure is mainly concentrated in the lower part. Although an obvious tensile crack (dashed lines) was generated in the lower part of the sample in a vertical direction after failure, numerous microcracks were equally observed due to the deformation and fracture of crystals in rock salt. That was the reason the distinct macroscopic failure surface was not obvious, even though the AE events were predominantly accumulated around the failure surface.

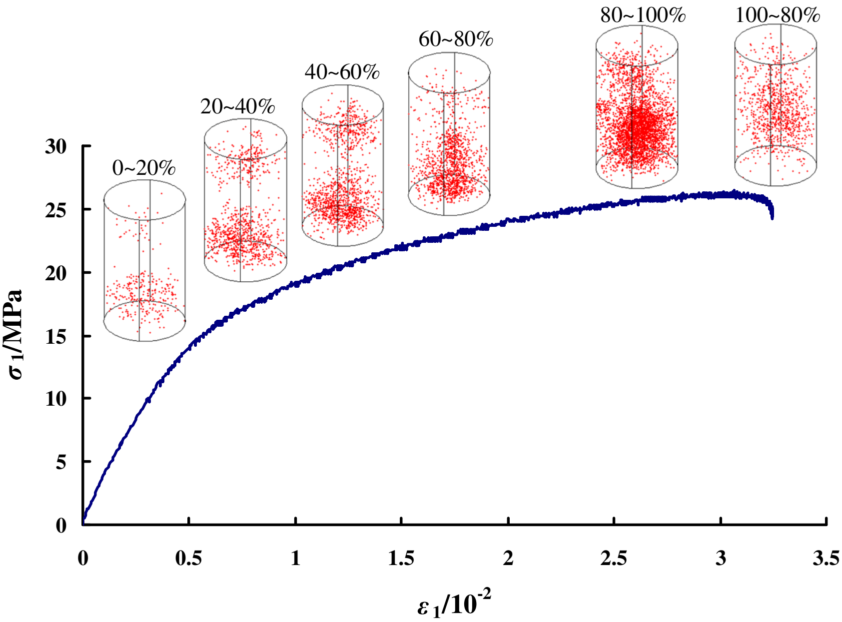

Fig. 4 Spatial distribution of AE events of rock salt for uniaxial compression test

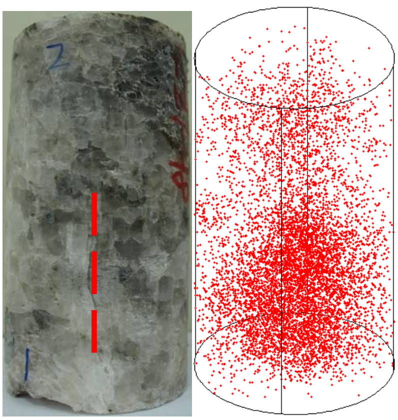

Fig. 5 Failure state and AE spatial distribution for uniaxial compression test

3.3 AE Events Properties for Triaxial Compression Tests

In triaxial compression tests, the AE events were recorded even during the hydrostatic loading process, as shown in Fig. 6. The distribution of AE events was somewhat arbitrary and similar to those recorded in the "100-80%" post-peak stage in Fig. 4. This can be attributed to the fact that the AE events were mainly induced by the closure of initial microcracks and defects under compressive stress in this phase. Since new microcracks were hardly generated in the hydrostatic loading process, the number of recorded AE events decreased with the increase of confining pressure. The results confirmed that the hydrostatic pressure is helpful in promoting the self-sealing process of microcracks in rock salt. Therefore, the self-sealing process of rock salt can be enhanced by increasing the hydrostatic pressure in the laboratory.

Compared to the distribution of AE events in uniaxial compression tests, significant differences can be noticed in triaxial compression tests. At the beginning of a triaxial compression test (0~20% of peak stress), even though the AE events were also essentially induced by the closure of initial microcracks and relative deformation between grains under uniaxial compressive stress, the end restraint effect was less evident than that under uniaxial compressive condition. As shown in Fig.7, the stress of yield deformation was about 40% of the peak stress. Therefore, the AE events were mainly located in the central and the lower part of the sample within 20~40% of peak stress. In this stress range, even though the closure of initial microcracks and relative deformation between grains in rock salt were still the main mechanisms responsible for the occurrence of AE events, the internal damage also starts to be initiated and to propagate. As a result, more AE events were recorded in this phase. When the axial stress exceeds 40% of the peak stress, the AE events were mainly generated by the relative deformation between grains and yield deformation. In the range of "40-60%", the AE events were concentrated in the central and upper part of the sample. With the increase in deviatoric stress ("80-100 %"), as a result of the significant plastic deformation and progressive damage development, the maximum number of AE events were captured in this range. In the post-failure regime (100-80%), due to the increase in the plastic deformation and damage evolution, considerable AE events are also recorded.

A special feature of crystallized soft rocks is that both the strength and deformation capacity of rock salt can be significantly increased by increasing the confining pressure. As shown in Fig. 7, the maximum axial deformation was almost 50%, i.e. about 16 times the deformation obtained in uniaxial compression tests. As a result, the original margin of internal grains becomes blurred, and no distinct failure surface is observed (Fig. 8(b)). Moreover, due to the non-uniform distribution of impurities and micro cracks in rock salt, the deformations of rock samples in vertical and lateral directions were not homogenous. The boundary of the deformed sample became uneven (Fig. 8(b)), and non-uniform spatial distribution of AE events in rock salt after failure was recorded (Fig. 8(c)).

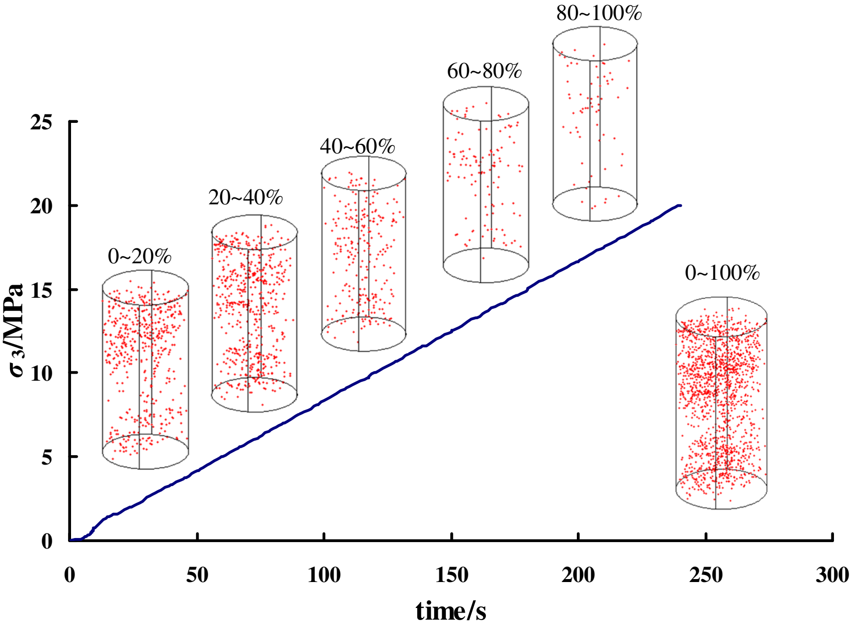

Fig. 6 Spatial distribution of AE events of rock salt under hydrostatic pressure condition

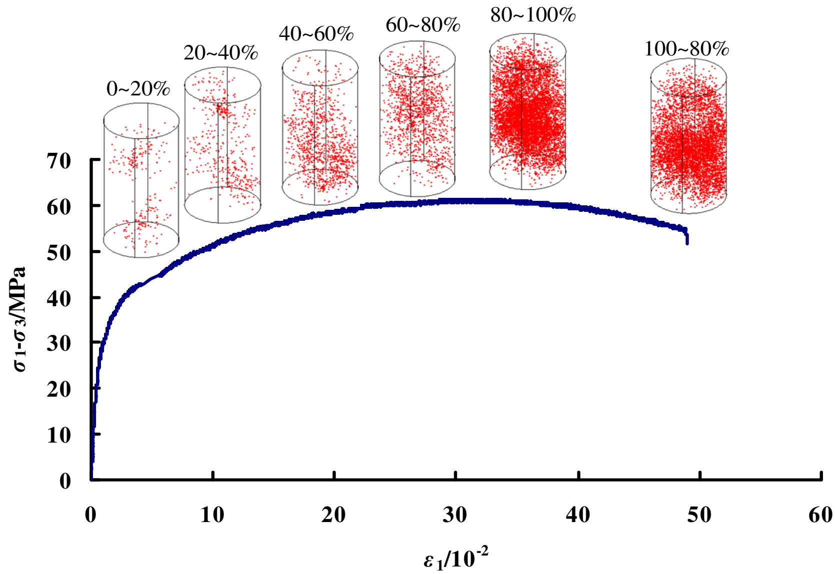

Fig. 7 Spatial distribution of AE events of rock salt for triaxial compression test (σ_3=20MPa)

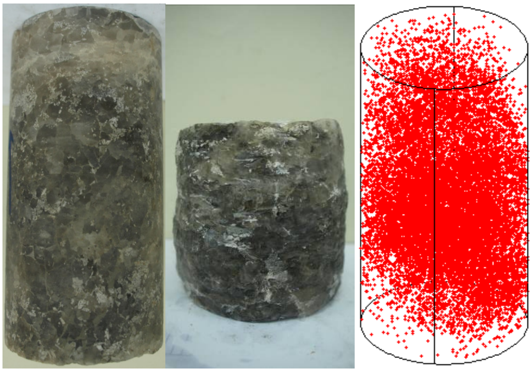

(a) before loading (b) after loading (c) location of acoustic emissions

Fig. 8 Failure state and AE spatial distribution for triaxial compression test (σ_3=20MPa)

4 Conclusions

The experimental results confirm that the stress condition had a significant influence on the spatial distribution of AE events during the whole loading process of salt rock. In indirect tensile tests, AE events were mainly generated along the loading surface at the beginning, and then expanded to the center of rock sample when the stress was increased. At the post-failure stage, the AE events were essentially related to the damage development around the failure surface.

Under uniaxial stress conditions, the distribution of AE events was strongly influenced by the end restraint effect. Before the rock failure, the AE events were essentially induced by the relative deformation between grains of rock salt, while the influence of damage development by macroscopic fracturing became more pronounced at the post-failure stage.

In triaxial compression tests, both in the hydrostatic phase and at the beginning of axial loading process, the closure of microcracks and the relative deformation between grains of rock salt might be the main mechanisms responsible for the occurrence of AE events. It was similar to the situation in uniaxial compression tests. However, the end restraint effect was less evident in triaxial compression tests. When the stress level exceeded the yield stress, the AE events were mainly induced by the relative deformation between grains and the further damage development.

In indirect tensile tests, a good consistency was obtained between the distribution of AE events and the orientation of the final failure surface. In contrast, due to the intensive microcrack formation, which was induced under a compressive stress condition and large plastic deformation, the accumulation of AE events along the single failure surface was not noticed in either uniaxial or triaxial compression tests.

Acknowledgement. The authors are grateful for the financial support from the National Natural Science Foundation of China (Grant No. 51120145001, 51104101, 51134018), the National Basic Research Projects of China (Grant No. 2011CB201201, 2010CB226802, and 2010CB732005), State Key Laboratory of Geohazard Prevention and Geoenvironment Protection (Grant No. SKLGP2013K016). The authors wish to offer their gratitude and regards to the colleagues who contributed to this work.

References

1. Hansen, F.D., Mellegard, K.D., Senseny, P.E.: Elasticity and strength of ten natural rock salt. In: Hardy Jr, H.R., Langer, M. (eds.) The first Conference on the Mechanical Behavior of Salt, pp. 71–83. Trans. Tech Publications (1984)
2. Hunsche, U.: Fracture experiments on cubic rock salt samples. In: Hardy Jr., H.R., Langer, M. (eds.) The First Conference on the Mechanical Behavior of Salt, pp. 169–179. Trans Tech Publications (1984)
3. Hunsche, U., Albrecht, H.: Results of true triaxial strength tests on rock salt. Engineering Fracture Mechanics 35(4/5), 867–877 (1990)
4. Hunsche, U., Plischke, I.: Stand der Untersuchungen zum Festigkeits-und Kriechverhalten von Steinsalz.6. Zwischenbericht zum Forschungsvorhaben SR 138 Gebirgsmechanik im Salz 1/81, Bundesanstalt für Geowissenschaften und Rohstoffe, Hannover. Archiv-Nr. 87952 (1981)
5. Farmer, I.W., Gilbert, M.J.: Dependent strength reduction of rock salt. In: Hardy Jr., H.R., Langer, M. (eds.) The First Conference on the Mechanical Behavior of Salt, pp. 4–18. Trans Tech Publications (1984)
6. Hunsche, U.: A failure criterion for natural polycrystalline rock salt. In: Fan, J., Murakami, S. (eds.) Advances in Constitutive Laws for Engineering Materials, pp. 1043–1046. International Academic Publ. (1989)
7. Skrotzki, W.: An estimate of the Brittle to ductile transition in salt. In: Hardy Jr., H.R., Langer, M. (eds.) The First Conference on the Mechanical Behavior of Salt, pp. 381–388. Trans Tech Publications (1984)
8. Obert, L., Duvall, W.I.: Use of subaudible noises for prediction of rockbursts II—report of investigation. S Bureau of Mines, Denver (1941)
9. Hodgson, E.A.: Velocity of elastic waves and structure of the crust in the vicinity of Ottawa, Canada. Bulletin of the Seismological Society of America 32(4), 249–255 (1942)
10. Kaiser, E.J.: A study of acoustic phenomena in tensile test. Dissertation Technical University, München (1950)
11. Li, C., Nordlund, E.: Experimental verification of the Kaiser effect in rocks. Rock Mechanics and Rock Engineering 26(4), 333–351 (1993)
12. Filimonov, Y.L., Lavrov, A.V., Shafarenko, Y.M., et al.: Memory effects in rock salt under triaxial stress state and their use for stress measurement in a rock mass. Rock Mechanics and Rock Engineering 34(4), 275–291 (2001)
13. Filimonov, Y.L., Lavrov, A.V., Shkuratnik, V., et al.: Acoustic emission in rock salt: effect of loading rate. Strain 38(4), 157–159 (2002)
14. Alkan, H., Cinary, Y., Pusch, G.: Rock salt dilatancy boundary from combined acoustic emission and triaxial compression tests. International Journal of Rock Mechanics and Mining Sciences 44(1), 108–119 (2007)

15. Liu, J., Xu, J., Yang, C., Hou, Z.: Mechanical characteristics of tensile failure of salt rock. Chinese Journal of Geotechnical Engineering 33(4), 580–586 (2011) (in Chinese)
16. Pei, J., Liu, J., Zhang, R., et al.: Fractal Study on Spatial Distribution of Acoustic Emission Events of Granite Specimens Under Uniaxial Compression. Journal of Sichuan University, Engineering Science Edition 42(6), 51–55 (2010) (in Chinese)
17. Ai, T., Zhang, R., Liu, J., et al.: Space- time evolution rules of acoustic emission locations under triaxial compression. Journal of China Coal Society 36(12), 2048–2057 (2011) (in Chinese)
18. The National Standards Compilation Group of People's Republic of China, GB/T50266-99 Standard for tests method of engineering rock masses. China Planning Press, Beijing (1999) (in Chinese)
19. The Professional Standard Compilation Group of People's Republic of China, SL264-2001 Specifications for rock tests in water conservancy and hydroelectric engineering. China Water Power Press, Beijing (2001) (in Chinese)
20. Zheng, Y., Zhang, H., Wang, Z., et al.: Experimental study on mechanical property of rock salt with impurity. Journal of China Coal Society 37(1), 17–20 (2012) (in Chinese)